Historical changes in drought characteristics and its impact on vegetation cover over Madagascar

Herijaona Hani-Roge Hundilida Randriatsara[1], Eva Holtanova[1], Karim Rizwan[2], Hassen Babaousmail[3], Mirindra Finaritra Tanteliniaina Rabezanahary[4], Kokou Romaric Posset[5], Donnata Alupot[6], Brian Odhiambo Ayugi[7]

[1]Department of Atmospheric Physics, Faculty of Mathematics and Physics, Charles University, Prague, V Holešovičkách 2, 18000, Prague 8, Czech Republic
[2]Key Laboratory of Meteorological Disaster, Ministry of Education (KLME)/Joint International Research Laboratory of Climate and Environment Change (ILCEC)/Collaborative Innovation Center on Forecast and Evaluation of Meteorological Disasters (CIC-FEMD), Nanjing, University of Information Science and Technology, Nanjing 210044, China
[3]School of Atmospheric Science and Remote Sensing, Wuxi University, Wuxi 214105, China
[4]Responsible people acting for development, Antananarivo 101, Madagascar
[5]Climate Change Department, Pan African University Institute for Water and Energy Sciences (Including Climate Change), C/O Université Abou Bekr Belkaid Tlemcen, Campus Chetouane, Tlemcen, Algeria
[6]Uganda National Meteorological Authority, plot 21, 28 portbell road Luzira-Kampala, P.O.Box 7025
[7]Department of Civil Engineering, Seoul National University of Science and Technology, Seoul 01811, Republic of Korea

Correspondence to: Herijaona Hani-Roge Hundilida Randriatsara (hundilida.randriatsara@matfyz.cuni.cz)

Abstract. Drought has become one of the most devastating natural hazards in recent decades causing severe vegetation degradation. This study aims to analyze the spatiotemporal characteristics of drought (duration, frequency, severity, intensity) over Madagascar during 1981-2022. In addition, it evaluates the relationship between the Standardized Precipitation Index (SPI) and the Normalized Difference Vegetation Index (NDVI) during 2000-2022, representing the impact of drought on vegetation over the studied area. Drought assessment was computed on SPI-3, SPI-6, and SPI-12 timescales, accompanied by seasonal and annual analyses. While the NDVI-SPI relationships were performed through the analysis of vegetation changes based on specific selected SPI time-periods and the correlation analysis. The findings reveal that drought events have become more consecutive during the most recent past (2017 to 2022) and intensified over the southern part of the country. Links between the drought occurrence and vegetation changes are confirmed: the occurrences of continuous negative values of seasonal and annual SPI increase vegetation losses, and the existence of smaller negative values of the wet season SPI relates to more vegetation degradation during the wet season. The correlation between NDVI and SPI emphasizes the NDVI-SPI relationship found with statistical significance, especially over southern Madagascar. These findings are crucial for complementing other climatic factors that influence Madagascar's vegetation besides drought.

1 Introduction

35   Drought has been identified as one of the gravest natural disasters experienced across the planet (Wilhite, 2000; Kalisa et al., 2020). Research has shown that droughts are some of the most damaging natural hazards, deteriorating means of living, including vegetation, due to its significant impacts on diverse sectors (Gouveia et al., 2017; Mbatha and Sifiso, 2018; Kannenberg et al., 2020; Lawal et al., 2021). Droughts are present across various climatic regions, including those with high and low precipitation levels, and are primarily linked to a prolonged decrease in rainfall over a specific period, such as a season

40   or a year (Mishra and Singh, 2010). Drought event can be categorized as; meteorological drought, caused by insufficient rainfall during a specific timeframe; hydrological drought, linked to the inadequate surface and groundwater availability; agricultural drought, resulting from a scarcity of water for plant growth; and socio-economic drought, which pertains to an inadequate supply to meet the demand for various economic commodities, encompassing the aforementioned three types of droughts (Heim, 2002; Udmale et al., 2014). According to the Intergovernmental Panel on Climate Change (IPCC), global

45   droughts are projected to intensify and occur more frequently worldwide due to climate change (IPCC, 2021).

        For the case of Madagascar, fewer studies have assessed drought events. Desbureaux and Damania (2018) assessed the impact of drought in inducing deforestation and degradation of biodiversity conservation over the country using the SPI method. However, the study lacks in-depth analysis of drought characteristics such as its frequency, its duration, its intensity, and its spatial patterns. As well as, Randriamarolaza et al. (2021) studied spatio-temporal drought characteristics in terms of

50   its magnitude and duration only by using the SPEI method. Moreover, their study presents some limitations such as the use of fewer station data that represent numerous missing values, and the dependency on data quality control and homogenization methods to complement these missing values. All of these might lead to some extent of uncertainties in the outputs. However, the Intergovernmental Panel on Climate Change Assessment Reports six (IPCC, 2021) reported that medium confidence level in the drought changes over Madagascar has been projected, mainly attributed to the lack of sufficient evidence. This calls for

55   an urgent need to conduct more in-depth studies over the country to identify the most affected regions by drought in terms of its full characteristics (duration, frequency, severity and intensity).

        Vegetation plays a vital role in natural ecosystems by managing the flow of water, carbon, and energy, offering habitats for various organisms, and ensuring global food and water security (Konduri et al., 2022). Droughts are widely recognized to cause diminishing of the primary and secondary productivity of vegetation and forests, triggering, among other

60   negative influences, the occurrence of tree mortality, and the loss of pastures (Smit et al., 2008; Bennett et al., 2015,). Southern Madagascar is currently facing severe food insecurity due to a significant drop in rice, maize, and cassava yields caused by the most severe drought in four decades, accompanied by sandstorms and pest invasions (Narvaez and Eberle, 2022). Studies have indicated that during drought, there is an observed rise in deforestation rates over Madagascar as farmers resort to clearing more forests to counter the adverse effects on agricultural productivity (Desbureaux and Damania, 2018). Assessing how

65   Madagascar's vegetation reacts to drought is crucial for understanding the susceptibility of the ecosystem on the island to extreme climatic events. Analyzing the historical patterns of drought and its effects on vegetation can offer valuable insights

for planning environmental, natural resource, and developmental strategies, pinpointing vulnerable ecosystems and livelihoods at risk of degradation or loss due to heightened drought conditions in the future. Thus, a comprehensive evaluation of the impact of drought events on natural ecosystems will offer insights into recent changes in vegetation to endure water scarcity
70 (Chaves et al., 2003; Kannenberg et al., 2020) and the complex interplay between the severity and duration of droughts in relation to their effects on vegetation (Vicente-Serrano et al., 201; Gouveia et al., 2017).

Choosing the right drought index is fundamental for identifying and defining droughts (Yao et al., 2018). This present study employs standard precipitation index (SPI) (McKee et al., 1993), not only because it is recommended by the World Meteorological Organization (WMO) to be used for drought analysis (Svoboda and Fuchs, 2017) but also because many studies
75 have successfully employed it in various regions (Elkollaly et al., 2018; Nkunzimana et al., 2021; Lawal et al., 2021; Nguyễn et al., 2023). Moreover, it has not been applied and studied so far over the Country. Besides, an appropriate index describing the vegetation cover must be used to investigate the impact of drought on vegetation. It is reported that the normalized difference vegetation index (NDVI) is the most extensively used vegetation index to investigate climate impacts on vegetation (Tian et al., 2015; Huang et al., 2021). This index has been successfully used and shown as a good indicator of vegetation
80 greenness, biomass, leaf area index, and primary production (Huete et al., 2002; Sun et al., 2011., Mbatha and Sifiso, 2018; Sharma et al., 2022). Out of the numerous vegetation indices, the NDVI is also a reliable measure for tracking vegetation status, commonly employed in monitoring land degradation, desertification, and often utilized for detecting and evaluating drought conditions (Zhao et al., 2018; Nanzad et al., 2019; Lawal et al., 2021). As an illustration, relationships between drought by using SPI method and vegetation indices including NDVI have been successfully evaluated over Africa (Vicente-Serrano
85 et al., 2013; Lawal et al., 2021). However, so far, any similar assessment of drought and its impacts on vegetation has not been performed over Madagascar**.**

Therefore, the aim of the present study is to evaluate the features of drought over Madagascar in recent decades from 1981 to 2022 and to assess the potential impact of selected drought episodes on vegetation. For the characterization of historical drought patterns and its effects on vegetation across Madagascar, this study employs SPI as the drought index and NDVI as
90 the vegetation index. The drought assessment is conducted on multiple SPI timescales accompanied by seasonal and annual analyses. Furthermore, it accounts for detailed examination in drought duration, frequency, severity and intensity. By connecting SPI and NDVI changes, the relationships between precipitation deficits and vegetation response could be explored.

2 Study area, data, and methods

2.1 Study Area

95 Madagascar is situated in the Indian Ocean, near the southeastern coast of Africa, within the coordinates of 12° - 25°S and 43° - 51°E, covering an area of approximately 592,040 km2 (Fig. 1). The country experiences two primary seasons: a hot-wet season from November to April and a cool-dry season from May to October (Jury et al., 1995; Randriamarolaza et al., 2021; Randriatsara et al., 2022a). These seasonal variations are primarily influenced by Madagascar's topography and geographical

location (Jury et al., 1995; Macron et al., 2016; Randriatsara et al., 2022a; Barimalala et al., 2018). Annual rainfall across the
100 country varies from 350 to 4000 mm, with a decreasing gradient from the eastern coast to the southwestern coast (Randriatsara
et al., 2022a, 2022b and 2023). Daily mean air temperature varies throughout the year from 23 to 27°C in coastal regions and
from 14 to 22°C in the central highlands. During the hot-wet season, the Inter-Tropical Convergence Zone (ITCZ) covers the
northern part of the country due to the convergence of the northwest monsoon wind and the trade winds (Randriamarolaza et
al., 2021), leading to rainfall across the whole of Madagascar except the southern parts. In contrast, these semi-arid southern
105 regions receive precipitation when the tropical temperate trough develops between November and February, extending from
Southern Africa to the Mozambique Channel (Macron et al., 2016; Barimalala et al., 2018). The southern region has low
vegetation cover and a dry steppe climate (Belda et al., 2014). In this study, we divided Madagascar into three regions (Fig. 1)
in accordance with the general land characteristics, the amount of rainfall, and the vegetation types. Region 1 (R1) is the
southern part of the country, the semi-arid area where the spiny forests reside. Region 2 (R2) is the western part covered by
110 dry forests (i.e., forests that can survive under a low amount of rain), while Region 3 (R3) is the eastern coast and represents
the tropical rainforest (Burgess et al., 2004; Desbureaux and Damania, 2018).
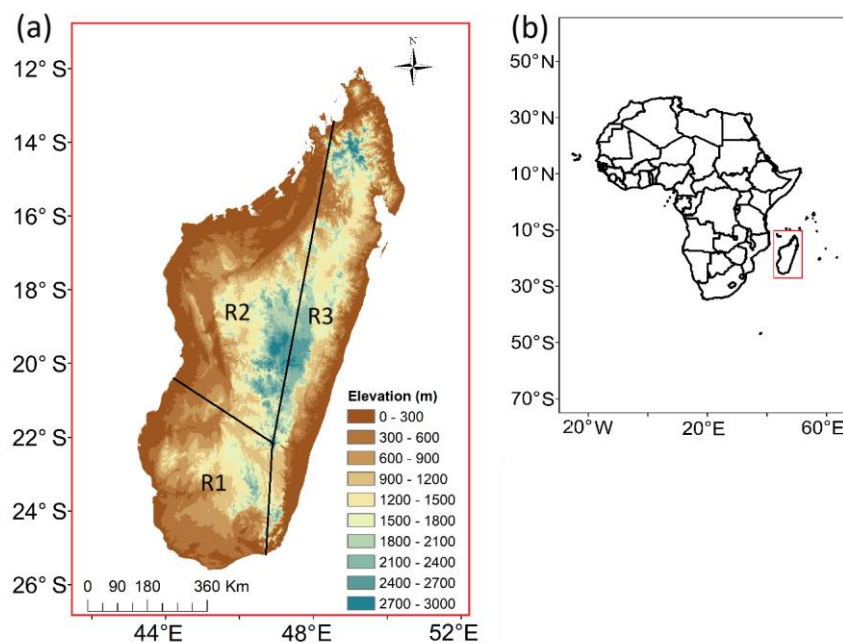
Figure 1: (a) Topographic map of the study area; and (b) geographical location of Madagascar (depicted in red rectangle) on the
115 **Africa map. R1 represents the southern region, R2 the western region and R3 the eastern region.**

2.2 Data

2.2.1 Precipitation data

The Climate Hazards Group InfraRed Precipitation with Station data (CHIRPS) is a valuable dataset for rainfall, covering a
120   wide geographical range from 50°S to 50°N and spanning the period from 1981 to near-present (Funk et al., 2015). Shalishe
et al. (2022) used CHIRPS v2.0 to assess drought characteristics in the Gamo Zone, Ethiopia, and found it to perform well.
Similarly, Li et al. (2023) demonstrated that CHIRPS effectively reproduced the spatial distribution of drought characteristics
in China's first-level water resource basins based on the standardized precipitation index (SPI). The CHIRPS v2.0 data is
available at https://iridl.ldeo.columbia.edu/SOURCES/.UCSB/.CHIRPS/.v2p0/.daily-improved/.global/.0p05/.prcp.

125   Further, the reanalysis ERA5 (Hersbach et al., 2020) is used for comparison. ERA5, as the fifth-generation
atmospheric reanalysis developed by ECMWF, integrates data from over 200 satellite instruments, as well as ground-based
radar-gauge data for rainfall (Hersbach et al., 2020). This dataset has proven valuable in the field of drought analysis
(Rakhmatova et al., 2021; Vicente-Serrano et al., 2022). Tladi et al. (2022) concluded that ERA5 outperforms other products
in monitoring drought characteristics in South Africa. The ERA5 dataset is available at
130   https://cds.climate.copernicus.eu/cdsapp#!/home.

       Both ERA5 and CHIRPS data exhibited good temporal and spatial performance in Madagascar from 1983 to 2015
(Randriatsara et al., 2022b). Combining CHIRPS v2.0 and ERA5 data offers a robust, enhanced dataset for comprehensive
analysis of drought characteristics in the study area. Both CHIRPSv2.0 and ERA5 datasets are selected for the period 1981 –
2022 for the current study, and all the results described below are based on the mean of these two datasets.

135   ### 2.2.2 Normalized Difference Vegetation Index (NDVI) data

NDVI represents the density of greenness over an area by referring to the reflectance in the near-infrared band (NIR) in
relationship to the reflectance in the visible shortwave radiation band (VIS) (Pettorelli et al., 2005). The VIS band is absorbed
by vegetation, while the vegetation reflects NIR. More reflected radiation in NIR wavelengths than in the VIS spectrum occurs
in dense vegetation. However, the difference between the magnitudes of the VIS and the NIR spectrum is small in sparse
140   vegetation. NDVI is defined as:

$$NDVI = \frac{(NIR-VIS)}{(NIR+VIS)},\tag{1}$$

       Theoretically, NDVI ranges from -1.0 to 1.0, although the realistic range is from 0.1 to 1.0 because, in the absence of
vegetation, NDVI is close to zero (Alex de la Iglesia Martinez and Labib, 2023). Slightly negative NDVI values have been
shown to depict differences in albedo (Alex de la Iglesia Martinez and Labib, 2023); however, these are mostly ignored. In
145   this present study, the NDVI is derived from Terra Moderate Resolution Imaging Spectroradiometer (MODIS) and represented
by Vegetation Indices Monthly MOD13C2 Version 6.1, with a spatial resolution of 0.05°. It covers the period 2000–present
day. More information about the data can be found in Didan (2021). The data are freely available at

https://lpdaac.usgs.gov/products/mod13c2v006/. The NDVI time series with monthly timestep were retrieved from EARTH DATA website by using AppEEARS tool (https://appeears.earthdatacloud.nasa.gov/).

150

2.3 Methods

2.3.1 Computation of the Standardized Precipitation Index (SPI)

The SPI is used here to assess the duration, frequency, severity, and intensity of drought and to identify anomalously dry periods. It is calculated as a standardized departure of observed precipitation from a theoretical probability distribution of the

155 precipitation for different time scales. In the present study, we focus on three (SPI-3), six (SPI-6), and twelve (SPI-12) months. Following McKee et al. (1993), the calculation is done by taking the difference of the precipitation from a mean for each particular time scale, which is then divided by the standard deviation. Previous studies define that the SPI-3, SPI-6 are normally used to assess agricultural and hydrological droughts, respectively, while the SPI-12 is important in studying groundwater droughts (Elkollaly et al., 2018; Nkunzimana et al., 2021). The classification of wet and dry conditions based on

160 the SPI values is shown in Table 1.

Table 1 Categories of dry and wet conditions based on SPI values following McKee et al. (1993)

SPI value	Category
≥ 2.00	Extremely wet
1.50 to 1.99	Severely wet
1.00 to 1.49	Moderately wet
- 0.99 to 0.99	Near normal
- 1.49 to - 1.00	Moderately dry
- 1.99 to - 1.50	Severely dry
≤ -2.00	Extremely dry

In this study, we applied a 2-parameter gamma distribution fit for SPI calculations (The NCAR Command Language, 2019). The gamma distribution parameters were estimated by the maximum likelihood method as described in Thom (1958).

165 ### 2.3.2 Computation of the SPI on the seasonal and annual scale

To evaluate the drought on a seasonal scale, SPI-6 of April of each year is used to represent the wet season (November-April) and SPI-6 of October for the dry season (May-October). This method was previously used by Elkollaly et al. (2018). Similarly, the same concept was applied for the annual scale by selecting the SPI-12 of December. In further text, we use the terms "seasonal SPI" and "annual SPI".

2.3.3 Drought characteristics - duration, frequency, severity, and intensity

The drought characteristics are calculated as follows:

- Drought duration means the sum of all the SPI values less than -1 (denoted as $SPI_{\leq -1}$) divided by the number of the events, i.e., the continuous occurrences of the SPI values less than -1:

$$Drought\ duration = \frac{Number\ of\ months\ with\ SPI_{\leq -1}}{Number\ of\ events}, \tag{2}$$

- Drought frequency is the percentage of the occurrence of the SPI values less than -1 throughout the study period

$$Drought\ frequency = \frac{Number\ of\ months\ with\ SPI_{\leq -1}}{Number_{Timesteps}} \times 100, \tag{3}$$

Where $Number_{Timesteps}$ is 504 months (the number of months in the study period).

- Drought severity refers to the sum of the SPI values less than -1 over all timesteps:

$$Drought\ severity\ = \sum SPI_{\leq -1}\ , \tag{4}$$

- Drought intensity refers to the average of the SPI values less than -1:

$$Drought\ intensity = \frac{|Drought\ severity|}{Number\ of\ months\ with\ SPI_{\leq -1}}, \tag{5}$$

2.3.3 Computation of correlation

In this study, we use both Pearson and Spearman correlations. The Pearson correlation measures the strength of the linear relationship between two variables (Wilks, 2006). Meanwhile, the Spearman correlation assesses the strength and direction of monotonic association between two variables. In other words, it is a calculation of Pearson correlation based on the ranked values of the data (Wilks, 2006).

3. Results

3.1 Temporal Evolution of SPI

3.1.1 Regional values of monthly SPI-3, SPI-6 and SPI-12

The SPI-3 (Fig. 2) shows that the occurrence of moderate to severe drought events (i.e. SPI values between -1 and -1.99) in the recent decade are more frequent over the southern region (R1) than over the western (R2) and eastern (R3) regions. The occurrence of extreme drought events (SPI values less than -2) is recorded scarcely in all regions. Extremely dry years were experienced during 1992, 2021 and 2022 over the R1, the years 1991 and 2017 over the R2, and the year 2017 over the R3. Similarly to SPI-3, the SPI-6 (Fig. 3) displays more occurrences of moderate and severe drought events over the R1 than the R2 and R3, especially in the recent decade. Figure 4 displays values of SPI-12 according to which continuous and longer

periods of dry events from moderate to severe levels are also observed over the southern region R1, while shorter periods and a smaller number of severe drought events occur over the R2 and R3. However, it is worth mentioning that based on SPI-12 all the regions experienced simultaneous drought in the years 1991, 2006, 2017, and 2021

3.1.2 Regional values of seasonal and annual SPI

200   Regarding the SPI for the wet season (SPI-6 for April, Fig. 5A), the results are very similar in R2 and R3 regions, where moderate drought events are noted during 1988, 1999, 2000, 2006, and 2017. However, in the years 1983 and 1992, R3 region experienced severe drought events followed by a continuous wetter period until the occurrence of moderate drought in 2010. By the end of the study period, between 2016 and 2022, the southern region R1 experienced consecutive drought. The temporal development of dry season SPI in Fig. 5B exhibits almost the same patterns in all three regions. The main features are the

205   occurrence of moderately to extremely wet years at the beginning of the study period from 1981 to 1986, and the weaker magnitude of SPI in dry years compared to wet years. The annual SPI (Fig. 5C) shows different years of moderate to extreme drought events over the three regions. However, it is worth mentioning that the region R1 experienced the most severe drought event in the year 2020.
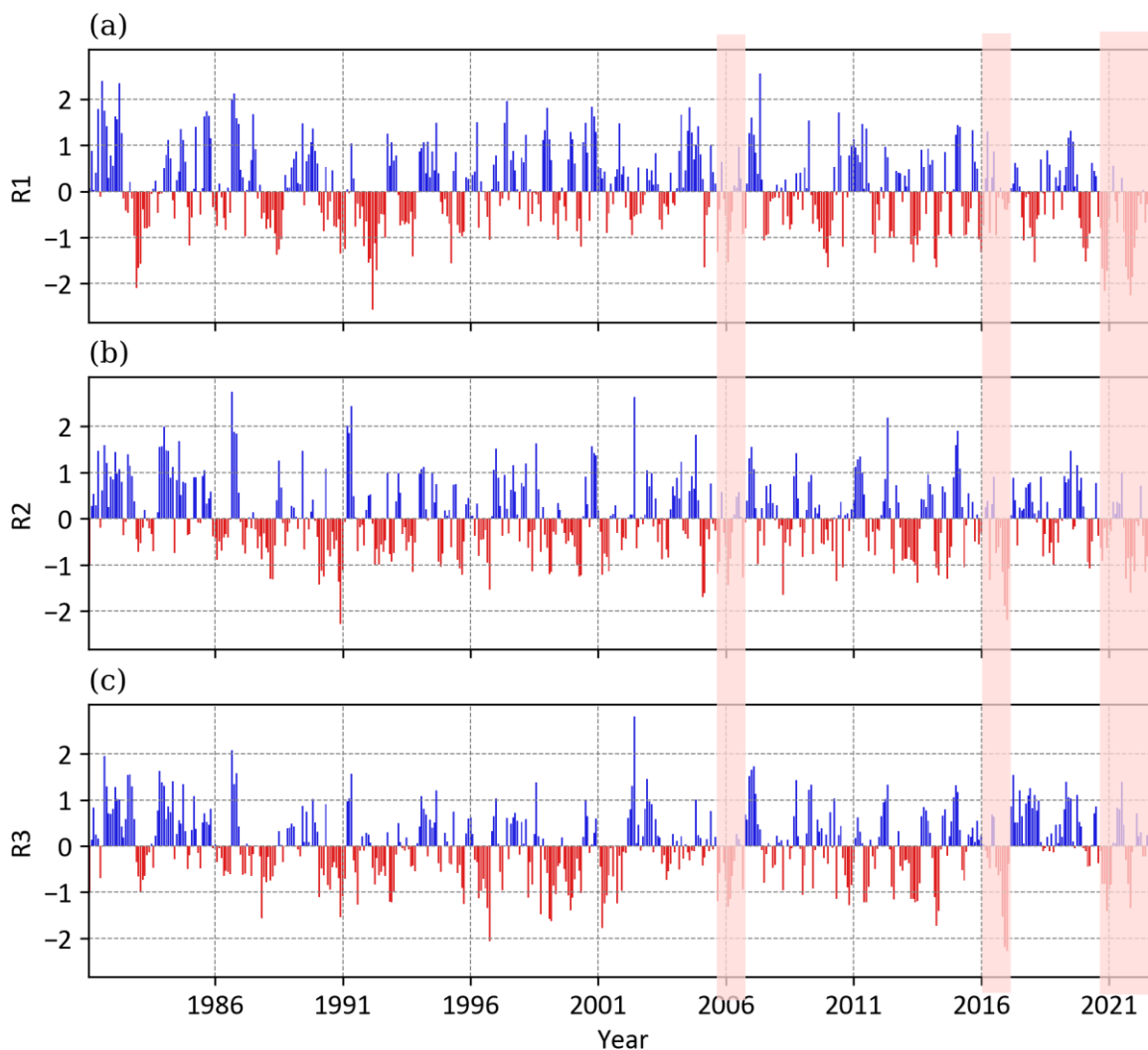
Figure 2: SPI-3 values from the ensemble mean of CHIRPS and ERA5 over Madagascar during the period 1981–2022 over different
regions of Madagascar. R1: South, R2: West and R3: East. The shaded areas represent selected periods which will be used for
analysis of connection between drought and vegetation.
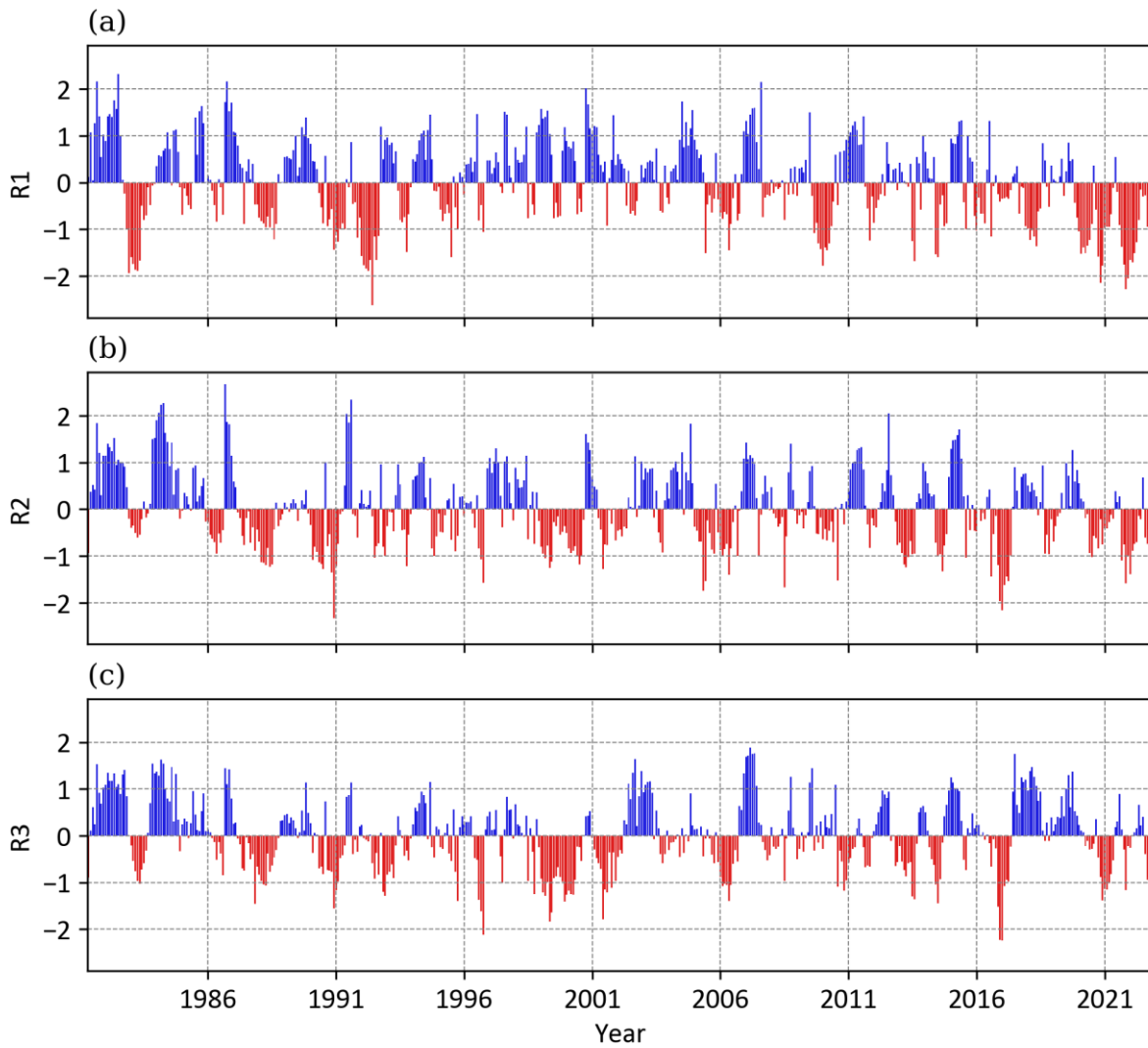
Figure 3: Same as Figure 2 but for SPI-6
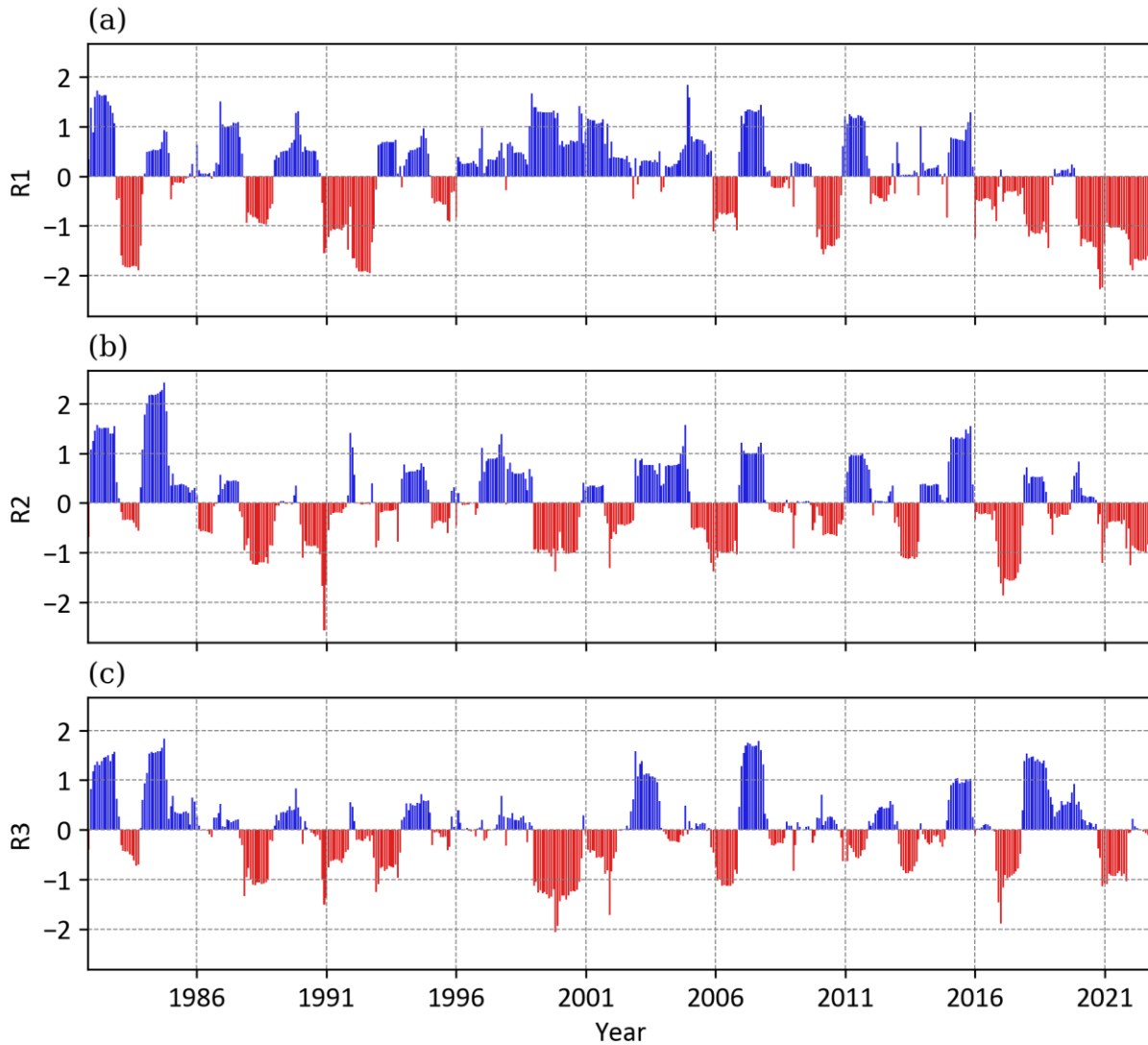
215

Figure 4: Same as Figure 2 but for SPI-12
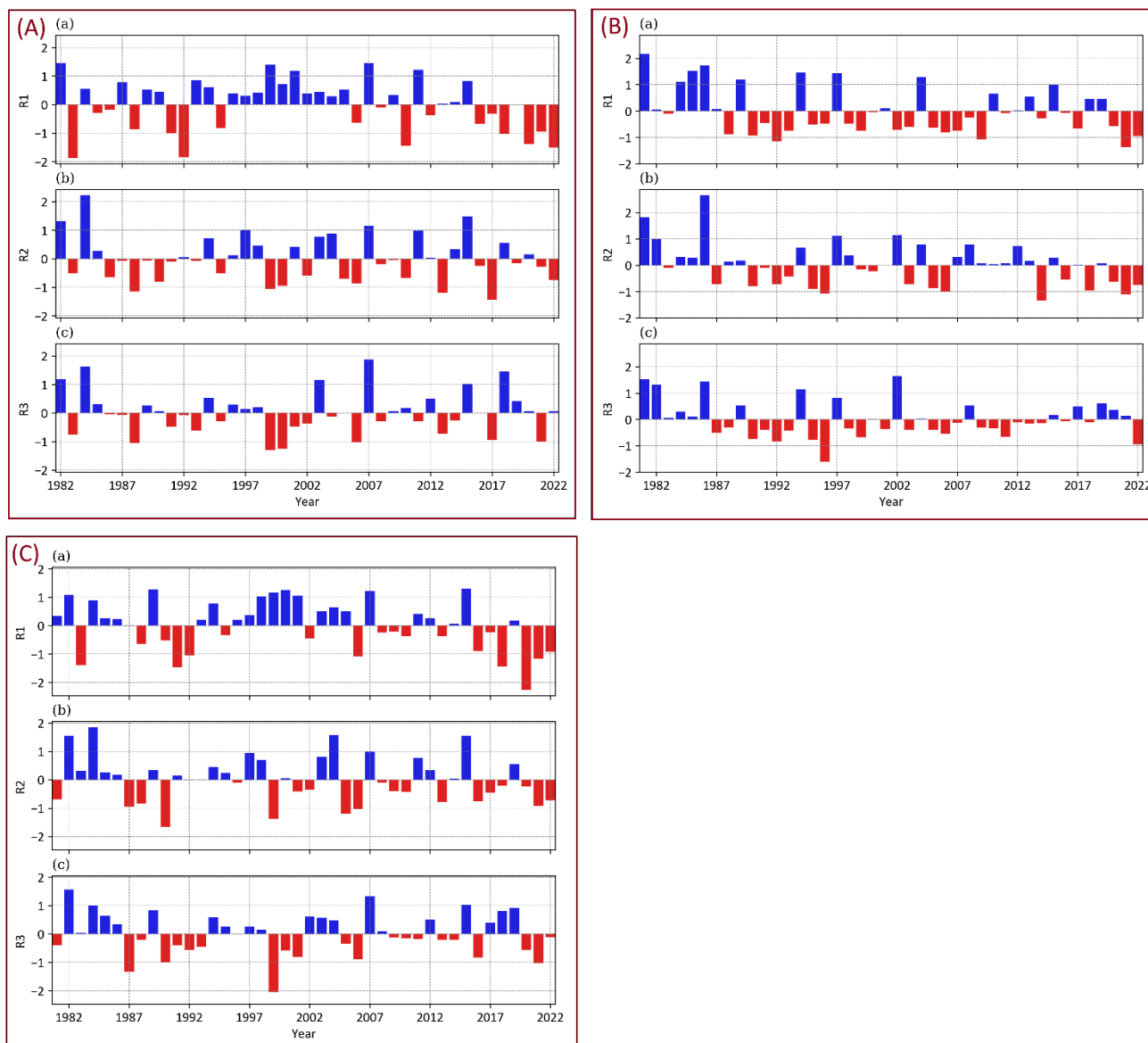
Figure 5: Same as Figure 2, but for (A) seasonal SPI representing the wet season (NDJFMA), (B) seasonal SPI representing the dry season (MJJASO), and (C) annual SPI.

3.2 Spatial analysis of drought characteristics (Duration, Frequency, Intensity, and Severity)

Figure 6 presents the spatial patterns of drought duration, frequency, intensity, and severity for SPI-3, SPI-6, SPI-12, and seasonal and annual scales. The longest drought duration is observed for SPI-12 (up to 26 months in the southern R1 region (Fig. 6c), while the shortest drought events are recorded for SPI-3 (2 months, Fig. 6a). Also, higher drought frequency is found for the longer timescale of SPI-12 (26%) compared to SPI-3 (about 17% Fig. 6g and 6i). Drought severity increases with

225 increasing time scale, with values from -85 to -115 for SPI-3, -105 to -125 SPI-6, and -125 to -165 SPI-12 (Fig. 6m, 6n, 6o). Less severe drought records are found over the western and some of the central parts of the country. Spatial patterns of drought intensity show homogeneous distribution of moderate drought events ranging from -1.3 ≥SPI> -1.9 for all the three timescales (3, 6 and 12 months, Fig. 6s, 6t, 6u). It is worth mentioning that for all the drought characteristics for all the three timescales, the magnitudes are higher over the southern region, especially for SPI-12, compared to the rest of the area.

230   Regarding the seasonal values, drought duration during the wet season NDJFMA in Fig. 6d and the dry season MJJASO in Fig. 6e show similar values of about 6.5 months with slightly higher duration over the southern region in the wet season. For the annual timescale, the drought duration shows marks of longer duration, up to ~11 months (Fig. 6f). Drought appears less frequently during the dry season (Fig. 6k) compared to the wet season (Fig. 6j). The annual frequency (Fig. 6l) reaches up to 24% over the south and the west of the country. The seasonal and annual values show higher spatial variability
235 of drought frequency and intensity than the SPI-3, -6, and -12 scales. The seasonal and annual drought severity reveal almost the same pattern, with values between –20 to –3 (Fig. 6p-6r). Drought intensity shows the occurrence of moderate drought during the dry season (Fig. 6w), while the wet season (Fig. 6v) and annual values (Fig. 6x) show severe to extreme drought events over most of the country except for the central-west part.

3.3 Potential causes of regional differences in drought characteristics and evolution

240 Overall, analysis implies that the southern region of Madagascar (R1) is more affected by drought events than the rest of the country, mainly for SPI-12 (Fig. 2, 3, 4, 5, 6). This region R1 is characterized by a semi-arid climate with annual rainfall of less than 800 mm/year and high annual mean air temperatures ranging between 23°C to 27 °C (Randriatsara et al., 2022a). Regarding potential causes of the above-described drought features, Huang et al. (2017) stated that globally, the largest warming was observed over the dry land, and the interdecadal variability in aridity changes are regulated by Ocean oscillations
245 which alter the changes in air temperature and rainfall. The impact of rainfall failure in 2019 to 2021 resulted in a severe food security crisis over southern Madagascar, compounded by the already straining impacts of COVID-19 and pest infestation (Harrington et al., 2022). According to Harrington et al. (2022), based on a combination of observations and climate modeling, the likelihood of poor rains experienced over the southern part of Madagascar was not found significantly increased due to human-caused climate change since it is overwhelmed by natural variability. However, a perceptible change in drought will
250 emerge over the region if anthropogenic activities increase the global mean temperatures by more than 2 °C above pre-industrial levels (IPCC 2021; Harrington et al., 2022). Other studies on the underlying processes responsible for the strong impact of drought duration and frequency over the southern parts of Madagascar reported an influence of ENSO, IOD, and sub-tropical IOD (SIOD) (Hoell et al., 2015; Hart et al., 2018; Barimalala et al., 2018; Randriatsara et al., 2022a). To illustrate, Randriatsara et al. (2022a) remarked that the enhanced (decreased) precipitation during wet (dry) years of the wet and dry
255 seasons in Madagascar is mainly linked to a strong moisture convergence (divergence) accompanied by strong easterlies (anticyclonic circulations) over the northwest (southern) Indian Ocean. The recent study of Barimalala et al. (2024) emphasized that the severe drought over the south of Madagascar in 2019 - 2021 was linked to the cold SST anomalies which were the

most negative anomalies (precisely the negative SIOD mode) in the past four decades during the rainy season of 2019 and 2020. All these mean that both the anthropogenic activities and the natural variability could have contributed to the drought
260 severity increase over the southern part of the Island.

Generally, drought characteristics across different regions of Africa reveal that Madagascar experiences the shortest drought duration for moderate, severe, and extreme drought categories compared to other climatic zones of Africa (Lim Kam Sian et al., 2023). However, the observed changes in drought characteristics during the recent past (1998 – 2017) are stronger over Madagascar than they were in the far past (1928–1957) (Tall et al., 2023). Moreover, this indicates that the drought events
265 have become more severe in recent years compared to earlier years in Madagascar. In support of that, this study reveals that drought occurrences have become more consecutive over the country, specifically from 2017 to 2022, and intensified over the southern part of the country. This finding aligns with the studies of Harrington et al. (2022) and Rigden et a.l (2024), which emphasized the increases in drought characteristics over southern Madagascar. Overall, the changes in drought events have been noted over different regions of the world (e.g. Sheffield et al., 2012; Cook et al., 2020) and Africa continent, with
270 numerous studies (e.g. Masih et al., 2014; Nooni et al., 2021; Ayugi et al., 2022; Lim Kam Sian et al., 2023) reporting the heterogeneous patterns of severity, intensity, duration of occurrence and frequencies.
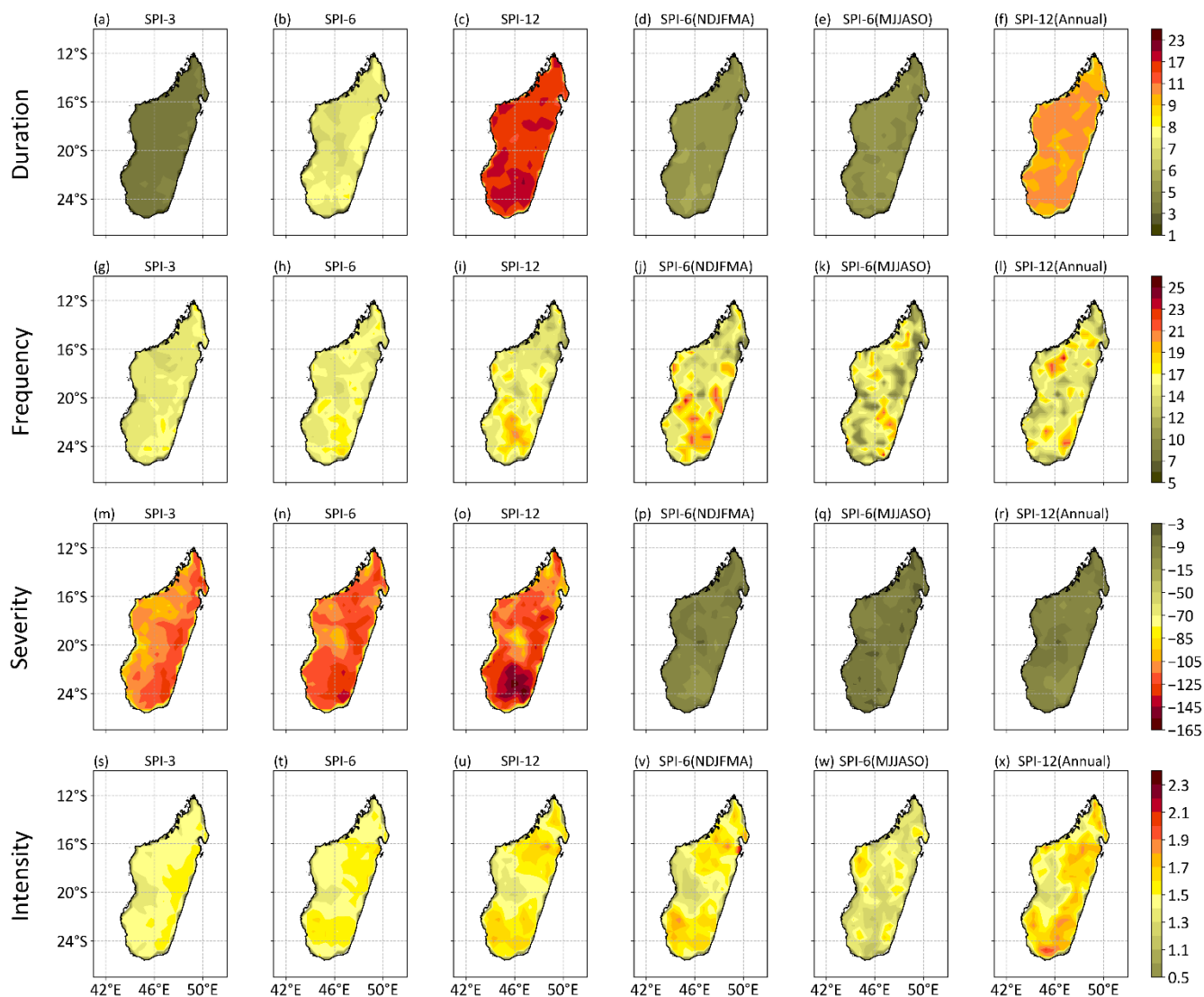
Figure 6: Spatial patterns of drought duration [months], frequency [%], severity and intensity on SPI-3, SPI-6, SPI-12, SPI-6 (NDJFMA), SPI-6 (MJJASO) and SPI-12 (Annual) scales.

3.4 Impact of drought on Vegetation

To compare NDVI in different months and locations, differences (anomalies) of individual NDVI values against their corresponding reference values of the year 2001 were performed. The year 2001 is chosen as a reference because not only does it represent normal conditions based on SPI values for the whole of Madagascar (Fig. S1 and S2 in the supplement), but also it appears as the earliest available NDVI data (See data section).

First, to study the impact of drought on vegetation, the three most severe drought episodes affecting the whole of Madagascar were selected. The selection was based both on the SPI values for each of the regions (Fig. 2), as well as the values for the whole island (Fig. S1). The episodes will be further denoted as "Event-I" (spanning October 2005-October 2006), "Event-II" (January 2016-April 2017), and "Event-III" (September 2020-December 2022).

3.4.1 NDVI differences based on the selected drought episodes

The anomaly of NDVI at the end of the Event-I (Fig. 7d) shows that the area with negative values has extended with an increased amplitude of up to -0.2 compared to the beginning of the event (Fig. 7a). This means that vegetation cover has decreased after the continuous occurrence of the negative SPI values during the Event-I, which agrees with our expectations. Surprisingly, the Event-II (Fig. 7b, 7e) shows contradictory outcomes, with the southern part of the island exhibiting more vegetation losses at the beginning of the event and enhanced vegetation at its ending. This is emphasized over the southern part of Madagascar, where the NDVI anomaly is up to -0.4 at the beginning of Event-II, but its magnitude decreases significantly by the end of the event (Fig. 7b, 7e). A noticeable increase in vegetation amounts up to 0.3 is also found over the eastern part of the country (Fig. 7b). Besides, Figure 7c shows a negative anomaly of the vegetation cover over almost the whole of Madagascar at the beginning of Event-III with values between -0.03 and -0.21. A decline of NDVI to -0.4 after the end of the drought episode is found only over the southern part of the country (Fig. 7f), and an increase with positive NDVI anomalies up to 0.24 is seen over the northern part. These surprising results can be, to some extent, explained considering the fact that the drought episodes have been chosen based on the SPI values for the whole island. However, in the different regions, the drought has a slightly different course, and therefore, naturally, the vegetation evolution differs.

Additional analyses were performed to comprehend the increase of vegetation cover during the Event-II (Fig. 7b, 7e). NDVI differences for each month of Event-II against the corresponding months of the reference year 2001 are shown in the additional Fig. S3. There is a peak of negative NDVI anomalies in January 2016, then the vegetation is recovering till October 2016. Then, the NDVI anomaly decreases from November 2016 to reach a negative peak in January 2017. Several other years were also analyzed (not shown here), and it was confirmed that the annual course is similar like in 2016, illustration for 2022 is shown in Fig. S4. This suggests that it is not appropriate to check the vegetation loss based on a single month by referring to the starting and ending months of the continuous occurrence of negative SPI values. This is because whenever the starting month falls in January and the ending month falls on other months, the intensity of vegetation loss is always greater, especially over the southern part. In addition, the changes in seasonal rainfall of Madagascar, such as the delaying and shortening of the rainy season in recent years over the southern part of the country (Harrington et al., 2022) have been found to influence vegetation's decline over the region (Rigden et al., 2024). This is obvious since the dry season of the country starts from May to October, however, the onset of the rainy season (November to April) over the southern region has delayed till December and January due to not only natural variability such as poleward migration of the mid-latitude jet (Rigden et al., 2024) but also the anthropogenic climate change (Dunning et al., 2018; Rigden et al., 2024). Therefore, it is unsurprising if the southern

region experiences the peak of vegetation loss in January, while the vegetation over northern and eastern regions has grown already.

However, it is worth mentioning that it is appropriate to analyze vegetation loss for a specific month from different years. For instance, more decline in vegetation cover is found in January 2022 (Fig. S4a) compared to January 2016 (Fig. S3a). This is relevant without the influence of seasonal rainfall and can be used to examine the impact of negative SPI values on vegetation changes for a specific month from different years.
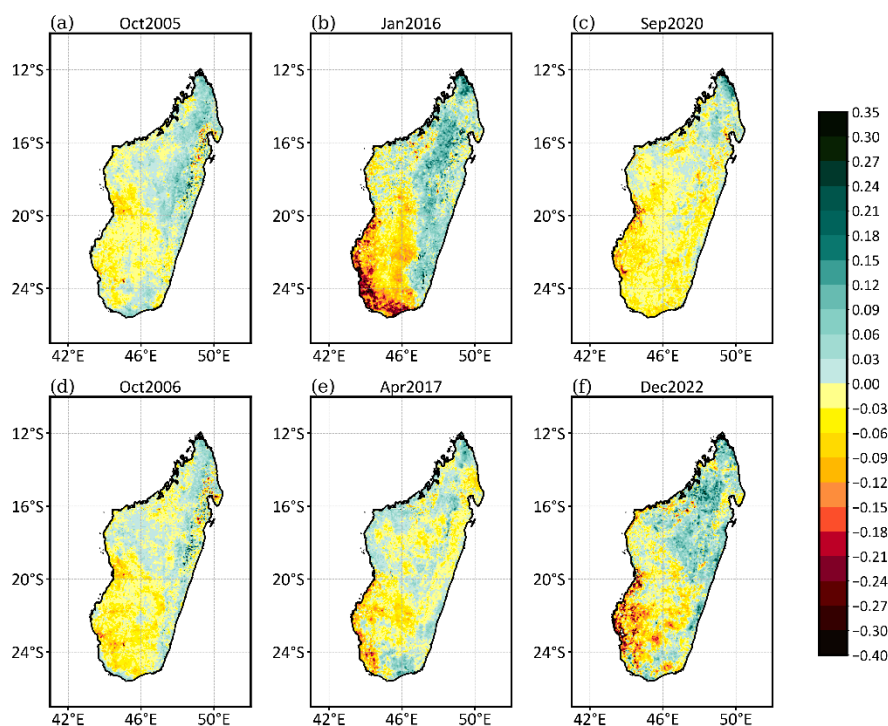
Figure 7: NDVI difference between selected months and their corresponding months from the reference year- 2001. The chosen months were based on the continuous occurrence of negative values found from the SPI-3, SPI-6 and SPI-12 as marked with shaded red rectangles in Fig. S1. a) and d) represent the difference at the beginning and the ending of the first occurrence of continuous negative SPI values, respectively. b) and e) represent the difference at the beginning and the ending of the second occurrence of continuous negative SPI values, respectively. c) and f) represent the difference at the beginning and the ending of the third occurrence of continuous negative SPI values, respectively.

3.4.2 Impact of drought in years selected based on seasonal and annual SPI

In this part, apart from Event-II, Event-I and Event-III are further analyzed since the continuous negative SPI values on seasonal and annual scales occur only for these two events (Fig. S2). Figure 8 presents annual mean NDVI anomalies for Event-I and Event-III. The Event-I starts in 2005 and ends in 2006 by referring to the annual and seasonal SPI in Fig. S2. The decrease in vegetation has intensified during this event. For instance, in 2005 the western part (between 16°S and 24°S) and

330   some of the central part of the country experienced negative NDVI anomalies of about -0.09, while the rest of the areas recorded positive values between 0.03 and 0.15 (Fig. 8c). By 2006, the decrease in vegetation extended to some of the northern region and the extreme southern part of the country with an increased NDVI amplitude of up to -0.15 (Fig. 8c). Similar patterns are found during Event-III occurring from 2020 to 2022 (Fig. 8b). In 2020, the southern region exhibited negative NDVI anomalies between -0.03 and -0.21 with a tiny spot of -0.27 over the south-west. Besides, positive anomalies of vegetation cover between

335   0.03 and 0.21 of NDVI were scattered over the north and east part of the country. However, by the end of the Event-III in 2022 (Fig. 8d), the areas with negative anomalies extended up to the northern part with increased values between -0.21 and -0.3 over several areas.

        These results suggest that the continuous occurrence of negative seasonal and annual SPI values (Fig. S2) enhances and spreads vegetation losses by the end of a drought event. In other words, the findings indicate that continuous negative

340   values of seasonal and annual SPI can be used to examine vegetation changes over Madagascar. This agrees with other studies (Nicholson et al., 1990; Camberlin et al., 2007; Zhang et al., 2023), which demonstrated that the inter-annual variations of the vegetation cover are correlated with annual and seasonal fluctuations of rainfall.
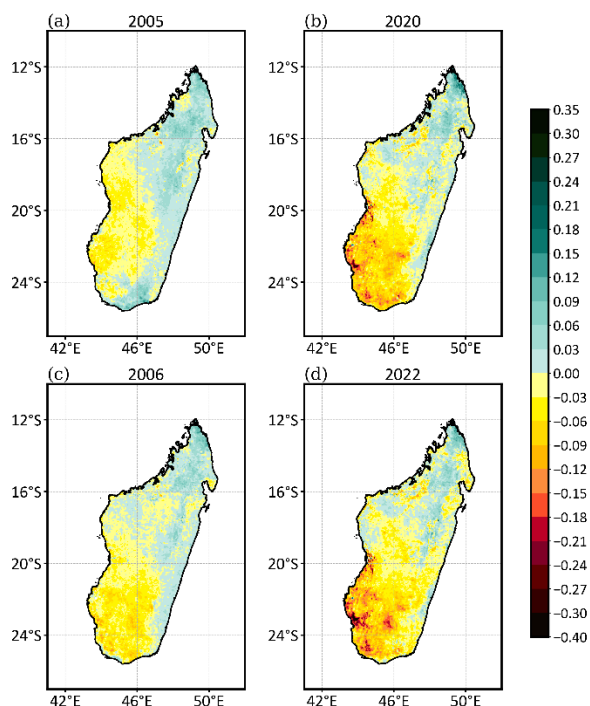
Figure 8: NDVI difference (anomaly) between selected years and the reference year 2001. The years are selected based on the

345   **continuous negative SPI values found during the seasonal analysis from Fig. S2 as marked with shaded rectangles. a) and c) represent the difference at the beginning and the ending of the first occurrence of continuous negative SPI values, respectively. b) and d) represent the difference at the beginning and the ending of the second occurrence of continuous negative SPI values, respectively.**

3.4.3 Vegetation response to the lowest values of wet season SPI

Another perspective on the impact of drought on vegetation is presented in Fig. 9, which shows seasonal and annual NDVI
350 anomalies for the years 2006, 2017 and 2021, chosen based on the lowest wet season SPI values (Fig. S3, marked with green
circles). The interest is only to analyze the wet season, to see the impact of rainfall scarcity on vegetation. The results show
that the smaller negative SPI amplitudes found in these selected years during the wet season (as marked in Fig. S2a) have huge
impacts on declining the wet season vegetation amounts (Fig. 9a, 9d, 9g) over the whole study area compared to the dry season
(Fig. 9b, 9e and 9h) and the annual scale (Fig. 9c, 9f, 9i). It is also worth mentioning that the intensity of the vegetation loss
355 during the wet season of these selected years has increased gradually from about -0.21 to -0.4 of NDVI, especially over the
southern part of the country. However, the dry season's vegetation (Fig. 9b, 9e, 9h) over most parts of the country has been
enhanced except over some parts of the south region. Besides, the vegetation changes for each averaged year (Fig. 9c, 9f, 9i)
show that more than half of the country experiences vegetation loss between -0.21 and -0.3 of NDVI with higher amplitude
values found in the southern part of the country.
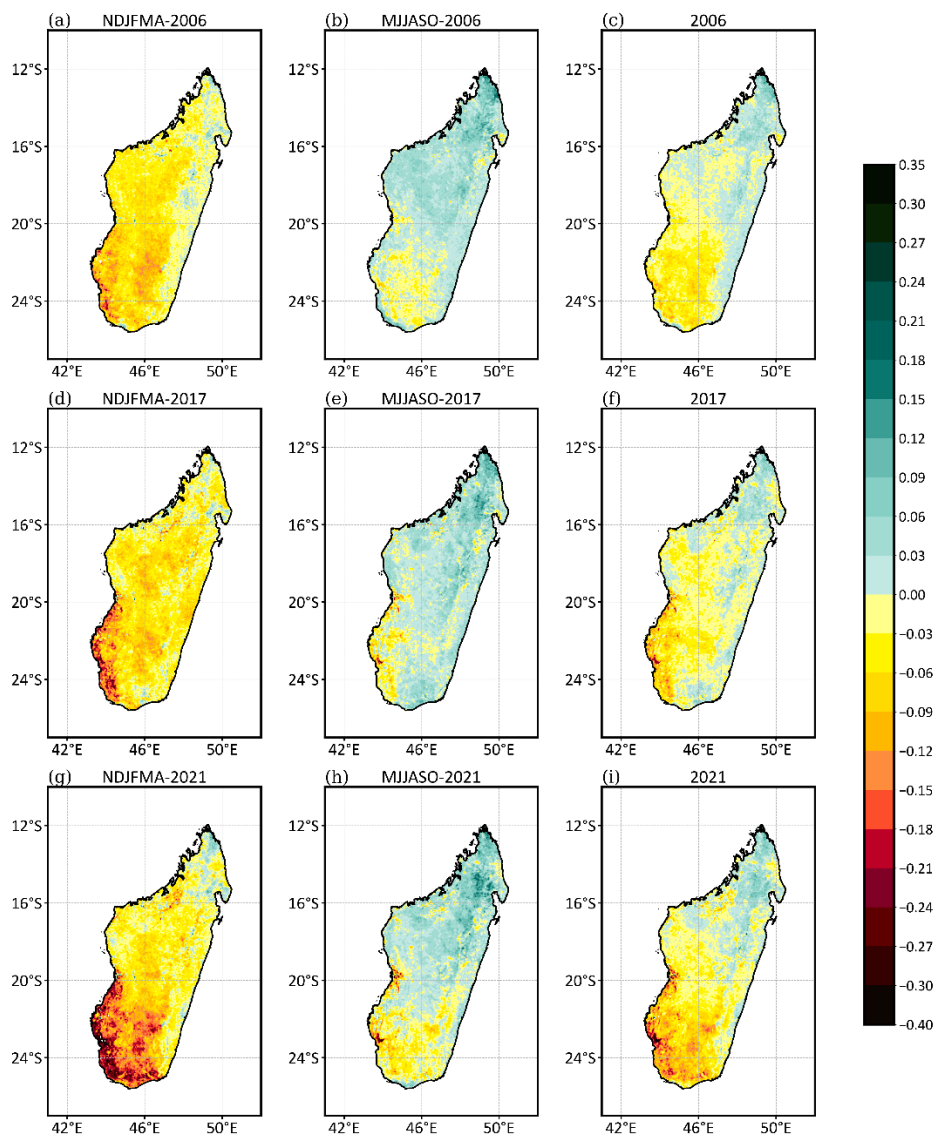
Figure 9: Seasonal NDVI difference between selected years and the reference year- 2001. The years 2006, 2017 and 2021 were chosen based on smaller negative values found during the wet season from Fig. S2a as marked with green circles. a), d), g) represent the differences during the wet season of each mentioned year. b), e), h) represent the differences during the dry season of each mentioned year. c), f), i) represent the differences for the annual averaged NDVI of each mentioned year.

The severe vegetation decrease found over southern Madagascar necessitated further analysis for the temporal development of annual mean NDVI in Fig. 10. Obviously, the highest NDVI values are seen for the eastern region (R3), which is the rainy forest region, followed by western region (R2), and the southern region (R1) with the lowest NDVI amounts. This clearly corresponds to the ecoregions and climatic types over Madagascar (Burgess et al., 2004; Desbureaux and Damania,

370 2018). Regarding the interannual variability, rather stable annual mean values of NDVI ranging from 0.62 to 0.66 (0.46-0.48)
are seen over the R3 (R2) region (Fig. 10). However, a considerable NDVI decline has occurred over the R1 region, with
decreasing values from 0.44 to 0.35 by the end of the study period (Fig. 10). To better detect this interannual NDVI decline
over southern Madagascar, temporal development of monthly NDVI values is performed in Fig. S5. It shows that the variability
over R2 and R3 is rather low even for the monthly values. However, the R1 region exhibits a noticeable vegetation decrease

375 from November to March (Fig. S5). The peak of the decline is captured in January, in which the NDVI is recorded to be about
0.55 in 2000 and reduced to about 0.32 in 2022. This severe decline found in January over southern Madagascar has been
explained earlier that it could be due to the delayed onset of the wet season rainfall over that region, which is caused by the
natural variability (Harrington et al., 2022; Rigden et al., 2024) and the anthropogenic climate change (Dunning et al., 2018;
Rigden et al., 2024). Moreover, these latter analyses (Fig. 10 and Fig. S5) show that the vegetation decline over the southern

380 region intensifies along with the most recent years. It has already been noticed above that the occurrence of drought has recently
become more frequent and intense. This could be among the reasons for the severe vegetation decline over the southern region
in the most recent years of the study period (see also 3.1).
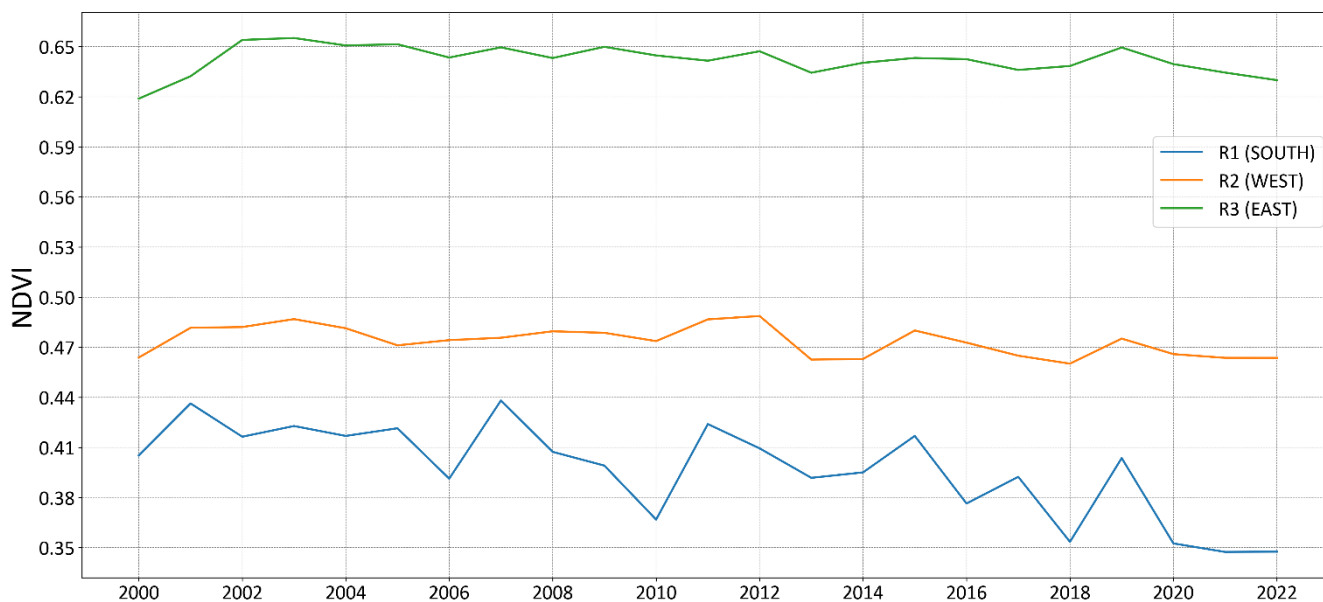
385 **Figure 10: Interannual variability of NDVI over different regions of Madagascar: R1: South, R2: West and R3: East.**

3.3.4 Correlation between SPI and NDVI

To assess the NDVI-SPI relationship in a quantitative way, we calculated correlations between the two variables over the
period 2000-2022. Temporal correlation analyses based on Pearson and Spearman methods (Fig. S6) were performed between

390   the NDVI and each SPI timescale (SPI-3, -6, and -12) over each region. The result shows positive correlation coefficient values over all the regions. However, it is worth mentioning that the southern region (R1) exhibits higher correlation coefficient values of about 0.26 to 0.29 compared to the regions R2 and R3 (between 0.05 and 0.19). This suggests that there is a connection between vegetation changes and the occurrence of drought events, while the connection is more emphasized over the southern region (R1) than over the two other regions. To better identify the connection, a spatial distribution of Pearson

395   correlation between NDVI and each SPI is performed in Fig. 11. For the case of SPI-3 and SPI-6 (Fig. 11a, 11b), more than half of the country exhibits a statistically significant correlation at 95% confidence level. But for the SPI-12, the correlation is only significant over the southern and some part of the northern region (Fig. 11c). It is worth mentioning that generally the correlation coefficient values are higher over the southern region compared to others. These findings reveal clearly that the changes in Madagascar's vegetation are linked to the rainfall anomalies, especially over the southern region (R1). Not only

400   drought is a direct factor that deteriorates vegetation of the Island, but also it leads to deforestation as farmers clear local forests to adverse its effects on agricultural productivity (Desbureaux and Damania, 2018). The latter could be among the reasons that amplifies higher positive correlation coefficients found between vegetation index and drought index over southern Madagascar (Fig. 11) due to the occurrence of more frequent and intense drought over that region. Moreover, Duku et al. (2021) reported that the significant human induced deforestation over local and non-local areas is among the factors that lead to a shortening

405   of the wet season rainfall over south Madagascar. This is obvious since deforestation has an indirect effect on trends in water availability by interacting with the atmosphere, as warming and drying tend to be caused by deforestation, resulting in precipitation decreases (Butt et al., 2011; Wright et al., 2017). Additionally, according to the reviews by Staten et al. (2020) and Xian et al., (2021), the expansion of Hadley cell in response to anthropogenic climate change leads to the drying condition of southern Madagascar. All of these factors which trigger precipitation reductions worsen vegetation losses over the southern

410   region compared to other regions of the country. On the other hand, the vegetation over western Madagascar shows weaker correlation with drought index for all the three SPI timescales. This could be due to the vegetation characteristic over the region, which is a dry forest able to survive even under dry conditions (Desbureaux and Damania, 2018; Lawal et al., 2021).
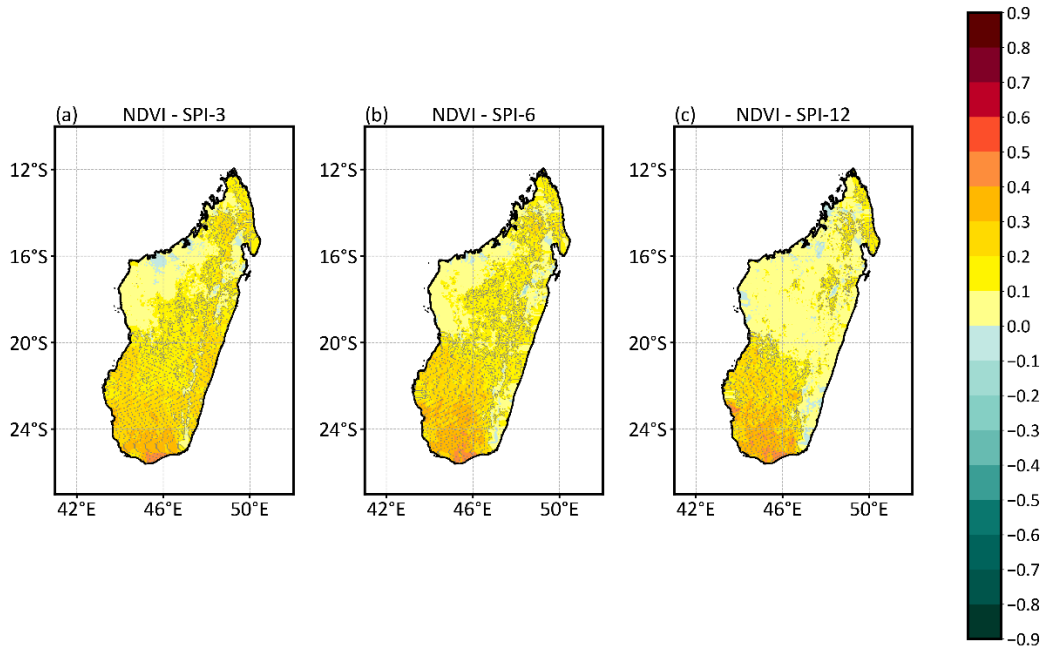
Figure 11: Spatial distribution of the Pearson correlation between NDVI and drought index for all three timescales
(SPI-3, -6, -12). Dotted areas are statistically significant at 95% confidence level using a student's t-test.

4. Conclusion

In summary, the aim of this study was twofold. Firstly, we analyzed the temporal development of SPI over Madagascar during
1981-2022 and the spatial distribution of the drought characteristics (duration, frequency, severity, intensity). Secondly, we
assessed the relationship between SPI and NDVI during 2000-2022, representing the impact of drought on vegetation over the
studied area.

 i)  This study reveals that drought occurrences have become more consecutive over the country, specifically
during the most recent past (2017 to 2022), and intensified over the southern part of the country. This finding
aligns with what has been found by Harrington et al. (2022), Tall et al. (2023), Rigden et al. (2024), and
Barimalala et al. (2024).

 ii)  The study also confirms that the occurrence of continuous negative values of seasonal and annual SPI (Fig.
S2) can be used to examine vegetation changes over Madagascar. The result shows that vegetation losses
have increased at the end of such occurrence. For instance, the years 2006 and 2022 (Fig. S2) are the ends
of the continuous occurrences of drought events, during which the decreases in vegetation cover are detected,
especially over the southern part of the country (Fig. 8). Similarly, smaller negative values of the wet season
SPI (Fig. S2a) can be employed to inspect vegetation losses during that season. The finding reveals that these

smaller SPI values have a huge impact on vegetation degradation of Madagascar during the wet season. For instance, the years 2006, 2017 and 2021 (Fig. S2a) represent smaller negative SPI values during the wet seasons, which display more vegetation losses over almost the whole country in these wet seasons compared to the dry seasons and the annual analyses (Fig. 9).

435   iii)   The relationship (quantified by the correlation) between vegetation and drought index is strongest over the southern and eastern part, whereas in the western part the correlation is lower. Among other reasons, we hypothesize that this could be due to different vegetation types. Dry forest over the western part of Madagascar is less vulnerable to drought than those of the southern and eastern. Moreover, the link found between more severe drought and vegetation losses over southern Madagascar (R1) compared to the western

440   (R2) and eastern (R3) regions could happen due to diverse factors that contribute to rainfall deficit over that region. These factors delay and shorten seasonal rainfall and are caused by both natural variability (Harrington et al., 2022; Rigden et al., 2024) and anthropogenic climate changes (Dunning et al., 2018; Rigden et al., 2024).

There are potentially other climatic factors influencing the vegetation besides drought, e.g., changes in air temperature
445 distribution and humidity, possibly connected to some large-scale circulation changes. Further, there are probably non-climatic anthropogenic factors, mainly deforestation and agricultural activities in the area. However, the analysis of these factors is beyond the scope of the present study and would be considered for the next research.

Code availability. Drought characteristics computation codes are available on request from the main author, Herijaona Hani-
450 Roge   Hundilida   Randriatsara.   The   SPI   calculation   is   available   on   the   NCL   website (https://www.ncl.ucar.edu/Applications/spi.shtml, NCAR Command Language).

Data availability. The ERA5 dataset is available on the Copernicus Climate Change Service (C3S) website at https://cds.climate.copernicus.eu/cdsapp#!/home.   The   CHIRPS   v2.0   data   is   available   at
455 https://iridl.ldeo.columbia.edu/SOURCES/.UCSB/.CHIRPS/.v2p0/.daily-improved/.global/.0p05/.prcp.   The   NDVI   time series with monthly timestep were retrieved from EARTH DATA website by using AppEEARS tool (https://appeears.earthdatacloud.nasa.gov/) and are freely available at https://lpdaac.usgs.gov/products/mod13c2v006/. The outputs data sets can be accessed through the reference Randriatsara et al. (2024).

460 *Author contributions.* Herijaona Hani-Roge Hundilinda Randriatsara: Conceptualization, data curation, formal analysis, methodology, original draft writing. Eva Holtanova: Conceptualization, Project administration, review and editing, supervision, funding acquisition, validation. Karim Rizwan: Data analysis, software and scripts. Hassen Babaousmail: Data analysis, software and scripts. Mirindra Finaritra Rabezanahary Tanteliniaina: Software and scripts. Kokou Romaric Posset:

Writing, review and editing. Donnata Alupot: Writing, review and editing. Brian Ayugi: Conceptualization, original draft
465   writing, review and editing.

Conflict of Interest. No convection-permitting conflict of interest amongst the authors.

Acknowledgment. The authors are grateful to the Johannes Amos Comenius Programme (P JAC) which supports this research,
470   as well as to the data centers for availing the datasets that were so instrumental in accomplishing the task.

Funding. This research was supported by the Johannes Amos Comenius Programme (P JAC) project No.
CZ.02.01.01/00/22_008/0004605, Natural and anthropogenic georisks.

References

475   Alex de la Iglesia Martinez, S. M. Labib: Demystifying normalized difference vegetation index (NDVI) for greenness exposure
assessments and policy interventions in urban greening, Environ. Res., 220, 115155,
https://doi.org/10.1016/j.envres.2022.115155, 2023.

Ayugi, B. O., Eresanya, E. O., Onyango, A. O., Ogou, F. K., Okoro, E. C., Okoye, C. O., Okenwa, E. O., Siyanbola, W. A.,
Maduako, R. E., and Akintoye, S. A.: Review of meteorological drought in Africa: historical trends, impacts, mitigation
480   measures, and prospects, Pure Appl. Geophys., 179, 1365-1386, https://doi.org/10.1007/s00024-022-02988-z, 2022.

Barimalala, R., Desbiolles, F., Blamey, R. C., and Reason, C.: Madagascar influence on the South Indian Ocean convergence
zone, the Mozambique Channel trough and Southern African rainfall, Geophys. Res. Lett., 45, 11380-11389,
https://doi.org/10.1029/2018GL079964, 2018.

Barimalala, R., Wainwright, C., Kolstad, E. W., Demissie, T. D.: The 2019–21 drought in southern Madagascar, Weather
485   Clim. Extrem., 46, 2212-0947, https://doi.org/10.1016/j.wace.2024.100723, 2024.

Belda, M., Holtanová, E., Halenka, T., and Kalvová, J.: Climate Classification Revisited: From Koppen to Trewartha, Clim.
Res., 59, 1-13, https://doi.org/10.3354/cr01204, 2014.

Bennett, A. C., McDowell, N. G., Allen, C. D., and Anderson-Teixeira, K. J.: Larger trees suffer most during drought in forests
worldwide, Nat. Plants, 1, 15139, https://doi.org/10.1038/nplants.2015.139, 2015.

490   Burgess, N., Hales, J., Underwood, E., Dinerstein, E., Olson, D., Itoua, I., Schipper, J., Ricketts, T., and Newman, K.:
Terrestrial eco-regions of Africa and Madagascar: A conservation assessment, World Wildlife Fund, ISBN: 1-55963-364-6,
https://www.researchgate.net/publication/292588815, 2004.

Butt, N., de Oliveira, P. A., and Costa, M. H.: Evidence that deforestation affects the onset of the rainy season in Rondonia,
Brazil, J. Geophys. Res. Atmos., 116, D11120, https://doi.org/10.1029/2010JD015174, 2011.

495 Camberlin, P., Martiny, N., Philippon, N., and Richard, Y.: Determinants of the interannual relationships between remote-sensed photosynthetic activity and rainfall in tropical Africa, Remote Sens. Environ., 106, 199-216, https://doi.org/10.1016/j.rse.2006.08.009, 2007.

Chaves, M. M., Maroco, J. P., and Pereira, J. S.: Understanding plant responses to drought from genes to the whole plant, Funct. Plant Biol., 30, 239-264, https://doi.org/10.1071/FP02076, 2003.

500 Cook, B. I., Mankin, J. S., Marvel, K., Williams, A. P., Smerdon, J. E., and Anchukaitis, K. J.: Twenty–first Century Drought Projections in the CMIP6 Forcing Scenarios, Earth's Future, 8, https://doi.org/10.1029/2019EF001461, 2020.

Desbureaux, S., and Damania, R.: Rain, forests and farmers: Evidence of drought-induced deforestation in Madagascar and its consequences for biodiversity conservation, Biol. Conserv., 217, 337-347, https://doi.org/10.1016/j.biocon.2018.03.005, 2018.

Didan, K.: MODIS/Terra Vegetation Indices Monthly L3 Global 0.05 Deg CMG, NASA EOSDIS LP DAAC,
505 https://lpdaac.usgs.gov/products/mod13c2v006/, last access: 10 September 2023.

Duku, C., and Hein, L.: The impact of deforestation on rainfall in Africa: a data-driven assessment, Environ. Res. Lett., 16, 064044, https://doi.org/10.1088/1748-9326/abfcfb, 2021.

Dunning, C. M., Black, E., and Allan, R. P.: Later wet seasons with more intense rainfall over Africa under future climate change, J. Clim., 31, 9719-9738, https://doi.org/10.1175/JCLI-D-18-0102.1, 2018.

510 Elkollaly, M., Khadr, M., and Zeidan, B.: Drought analysis in the Eastern Nile basin using the standardized precipitation index, Environ. Sci. Pollut. Res., 25, 10265-10278, https://doi.org/10.1007/s11356-016-8347-9, 2018.

Funk, C., Peterson, P., Landsfeld, M., Pedreros, D., Verdin, J., Shukla, S., Husak, G., Rowland, J., Harrison, L., Hoell, L., and Michaelsen, J.: The climate hazards infrared precipitation with stations - A new environmental record for monitoring extremes, Sci. Data, 2, 150066, https://doi.org/10.1038/sdata.2015.66, 2015.

515 Gouveia, C. M., Trigo, R. M., Beguería, S., and Vicente-Serrano, S. M.: Drought impacts on vegetation activity in the Mediterranean region: An assessment using remote sensing data and multi-scale drought indicators, Glob. Planet. Change, 151, 15-27, https://doi.org/10.1016/j.gloplacha.2016.06.011, 2017.

Harrington, L. J., Wolski, P., Pinto, I., Ramarosandratana, A. M., Barimalala, R., Vautard, R., Philip, S., Kew, S., Singh, R., Heinrich, D., Arrighi, J., Raju, E., Thalheimer, L., Razanakoto, T., Aalst, M., Li, S., Bonnet, R., Yang, W., Otto, F., and
520 Oldenborgh, G.: Limited role of climate change in extreme low rainfall associated with southern Madagascar food insecurity, 2019–21, Environ. Res. Clim., 1, 021003, https://doi.org/10.1088/2752-5295/aca695, 2022.

Hart, N. C., Washington, R., and Reason, C. J. C.: On the likelihood of tropical–extratropical cloud bands in the South Indian convergence zone during ENSO events, J. Clim., 31, 2797-2817, https://doi.org/10.1175/JCLI-D-17-0221.1, 2018.

Heim, R. R. Jr.: A review of twentieth-century drought indices used in the United States, Bull. Am. Meteorol. Soc., 83, 1149-
525 1166, https://doi.org/10.1175/1520-0477-83.8.1149, 2002.

Hersbach, H., Bell, B., Berrisford, P., Hirahara, S., Horányi, A., Muñoz-Sabater, J., Nicolas, J., Peubey, C., Radu, R., Schepers, D., Simmons, A., Soci, C., Abdalla, S., Abellan, X., Balsamo, G., Bechtold, P., Biavati, G., Bidlot, J., Bonavita, M., Chiara, G. D., Dahlgren, P., Dee, D., Diamantakis, M., Dragani, R., Flemming, J., Forbes, R., Fuentes, M., Geer, A., Haimberger, L.,

Healy, S., Hogan, R. J., Hólm, E., Janisková, M., Keeley, S., Laloyaux, P., Lopez, P., Lupu, C., Radnoti, G., De Rosnay, P.,

530   Rozum, I., Vamborg, F., Villaume, S., and Thépaut, J.: The ERA5 global reanalysis, Q. J. R. Meteorol. Soc., 146, 1999–2049, https://doi.org/10.1002/qj.3803, 2020.

Hoell, A., Funk, C., Magadzire, T., Zinke, J., and Husak, G.: El Nino–Southern Oscillation diversity and Southern Africa teleconnections during Austral Summer, Clim. Dyn., 45, 1583–1599, https://doi.org/10.1007/s00382-014-2414-z, 2015.

Huang, J., Li, Y., Fu, C., Chen, F., Fu, Q., Dai, A., Shinoda, M., Ma, Z., Guo, W., Li, Z., Zhang, L., Liu, Y., Yu, H., He, Y.,

535   Xie, Y., Guan, X., Ji, M., Lin, L., Wang, S., Yan, H., and Wang, G.: Dryland climate change: Recent progress and challenges, Rev. Geophys., 55, 719–778, https://doi.org/10.1002/2016RG000550, 2017.

Huang, S., Tang, L., Hupy, J. P., Wang, Y., and Shao, G.: A commentary review on the use of normalized difference vegetation index (NDVI) in the era of popular remote sensing, J. For. Res., 32, 1–6, https://doi.org/10.1007/s11676-020-01155-1, 2021.

Huete, A., Didan, K., Miura, T., Rodriguez, E. P., Gao, X., and Ferreira, L. G.: Overview of the radiometric and biophysical

540   performance of the MODIS vegetation indices, Remote Sens. Environ., 83, 195–213, https://doi.org/10.1016/S0034-4257(02)00096-2, 2002.

IPCC: Summary for policymakers, in: Climate Change 2021 – The physical science basis: Working Group I contribution to the sixth assessment report of the Intergovernmental Panel on Climate Change, Cambridge University Press, 3–32, https://doi.org/10.1017/9781009157896.001, 2021.

545   Jury, M., Parker, B. A., Raholijao, N., and Nassor, A.: Variability of summer rainfall over Madagascar: Climatic determinants at interannual scales, Mon. Weather Rev., 15, 1323–1332, https://doi.org/10.1175/MWR-D-15-0077.1, 1995.

Kalisa, W., Zhang, J., Igbawua, T., Ujoh, F., Ebohon, O. J., and Namugiza, J.: Spatio-temporal analysis of drought and return periods over the East African region using Standardized Precipitation Index from 1920 to 2016, Agric. Water Manag., 237, 106195, https://doi.org/10.1016/j.agwat.2020.106195, 2020.

550   Kannenberg, S. A., Schwalm, C. R., and Anderegg, W. R. L.: Ghosts of the past: How drought legacy effects shape forest functioning and carbon cycling, Ecol. Lett., 23, 891–901, https://doi.org/10.1111/ele.13485, 2020.

Konduri, V. S., Morton, D. C., and Andela, N.: Tracking changes in vegetation structure following fire in the Cerrado biome using ICESat-2, J. Geophys. Res. Biogeosci., 128, e2022JG007046, https://doi.org/10.1029/2022JG007046, 2023.

Lawal, S., Hewitson, B., Egbebiyi, T. S., and Adesuyi, A.: On the suitability of using vegetation indices to monitor the response

555   of Africa's terrestrial ecoregions to drought, Sci. Total Environ., 792, 148282, https://doi.org/10.1016/j.scitotenv.2021.148282, 2021.

Li, Y., Zhuang, J., Bai, P., Yu, W., Zhao, L., Huang, M., and Xing, Y.: Evaluation of three long-term remotely sensed precipitation estimates for meteorological drought monitoring over China, Remote Sens., 15, 154, https://doi.org/10.3390/rs15010086, 2023.

560   Narvaez, L., and Eberle, C.: Southern Madagascar food insecurity, Interconnected Disaster Risks, UNU-EHS Reports, 2021/2022, https://doi.org/10.53324/JVWR3574, 2022.

Lim Kam Sian, K. T., Zhi, X., Ayugi, B. O., Onyutha, C., Shilenje, Z. W., and Ongoma, V.: Meteorological drought variability over Africa from multisource datasets, Atmosphere, 14, 1052, https://doi.org/10.3390/atmos14061052, 2023.

Macron, C., Richard, Y., Garot, T., Bessafi, M., Pohl, B., Ratiarison, A., and Razafindrabe, A.: Intraseasonal rainfall variability over Madagascar, Mon. Weather Rev., 144, 1877–1885, https://doi.org/10.1175/MWR-D-15-0077.1, 2016.

Pettorelli, N., Vik, J. O., Mysterud, A., Gaillard, J.-M., Tucker, C. J., and Stenseth, N. C.: Using the satellite-derived NDVI to assess ecological responses to environmental change, Trends Ecol. Evol., 20, 503–510, https://doi.org/10.1016/j.tree.2005.05.011, 2005.

McKee, T. B., Doesken, N. J., and Kleist, J.: The relationship of drought frequency and duration to time scales, in: Proceedings of the 8th Conference on Applied Climatology, Anaheim/Canada, 17–23 January, 179–184, 1993.

Mishra, A. K., and Singh, V. P.: A review of drought concepts, J. Hydrol., 391, 202–216, https://doi.org/10.1016/j.jhydrol.2010.07.012, 2010.

Masih, I., Maskey, S., Mussá, F. E. F., and Trambauer, P.: A review of droughts on the African continent: A geospatial and long-term perspective, Hydrol. Earth Syst. Sci., 18, 3635–3649, https://doi.org/10.5194/hess-18-3635-2014, 2014.

Nanzad, L., Zhang, J., Tuvdendorj, B., Nabil, M., Zhang, S., and Bai, Y.: NDVI anomaly for drought monitoring and its correlation with climate factors over Mongolia from 2000 to 2016, J. Arid Environ., 164, 69–77, https://doi.org/10.1016/j.jaridenv.2019.01.019, 2019.

Nguyễn, Q. T., Govind, A., Le, M. H., Nguyen, T. M. L., Linh, N. T. M., Anh, T. M. T., Hai, N. K., and Ha, T. V.: Spatiotemporal characterization of droughts and vegetation response in Northwest Africa from 1981 to 2020, Egyptian J. Remote Sens. Space Sci., https://doi.org/10.1016/j.ejrs.2023.05.006, 2023.

Nicholson, S. E., and Kim, J.: The relationship of the El Niño-Southern Oscillation to African Rainfall, Int. J. Climatol., 17, 117–135, https://doi.org/10.1002/(SICI)1097-0088(199702)17:2<117::AID-JOC84>3.0.CO;2-O, 1997.

Mbatha, N., and Sifiso, X.: Time series analysis of MODIS-derived NDVI for the Hluhluwe-Imfolozi Park, South Africa: Impact of recent intense drought, Climate, 6, 95, https://doi.org/10.3390/cli6040095, 2018.

Nkunzimana, A., Shuoben, B., Guojie, W., Alriah, M. A. A., Sarfo, I., Zhihui, X., Vuguziga, F., and Ayugi, B. O.: Assessment of drought events, their trend and teleconnection factors over Burundi, East Africa, Theor. Appl. Climatol., 145, 1293–1316, https://doi.org/10.1007/s00704-021-03680-3, 2021.

Nooni, I. K., Hagan, D. F. T., Wang, G., Ullah, W., Li, S., Lu, J., and Zhu, C.: Spatiotemporal characteristics and trend analysis of two evapotranspiration-based drought products and their mechanisms in sub-Saharan Africa, Remote Sens., 13, 533, https://doi.org/10.3390/rs13030533, 2021.

Rakhmatova, N., Arushanov, M., Shardakova, L., Nishonov, B., Taryannikova, R., Rakhmatova, V., and Belikov, D. A.: Evaluation of the perspective of ERA-Interim and ERA5 reanalyses for calculation of drought indicators for Uzbekistan, Atmosphere, 12, https://doi.org/10.3390/atmos12050527, 2021.

Randriamarolaza, L. Y. A., Aguilar, E., Skrynyk, O., Sergio, M., Vicente-Serrano, and Domínguez-Castro, F.: Indices for daily
temperature and precipitation in Madagascar, based on quality-controlled and homogenized data, 1950-2018, Int. J. Climatol.,
42, 265-288, https://doi.org/10.1002/joc.7243, 2021.

Randriatsara, H. H. -R. H., Hu, Z., Ayugi, B., Makula, E. K., Vuguziga, F., and Nkunzimana, A.: Interannual characteristics
of rainfall over Madagascar and its relationship with the Indian Ocean sea surface temperature variation, Theor. Appl.
Climatol., 148, 349–362, http://dx.doi.org/10.1007/s00704-022-03950-8, 2022a.

Randriatsara, H. H. -R. H., Hu, Z., Xu, X., Ayugi, B., Sian, K. T. C. L. K., Mumo, R., and Ongoma, V.: Evaluation of gridded
precipitation datasets over Madagascar, Int. J. Climatol., 42, 7028–7046, http://dx.doi.org/10.1002/joc.7628, 2022b.

Randriatsara, H. H. -R. H., Hu, Z., Xu, X., Ayugi, B., Sian, K. T. C. L. K., Mumo, R., Ongoma, V., and Holtanova, E.:
Performance evaluation of CMIP6 HighResMIP models in simulating precipitation over Madagascar, Int. J. Climatol.,
http://dx.doi.org/10.1002/joc.8153, 2023.

Randriatsara, H. H.-R. H., Holtanová, E., Rizwan, K., Babaousmail, H., Rabezanahary, M. F. T., Posset, K. R., Alupot, D., &
Brian Odhiambo, A.: Historical changes in drought characteristics and its impact on vegetation cover over Madagascar [Data
set]. Zenodo. https://doi.org/10.5281/zenodo.13768972, 2024.

Rigden, A., Golden, C., Chan, D., and Huybers, P.: Climate change linked to drought in Southern Madagascar, Clim. Atmos.
Sci., 7, 41, https://doi.org/10.1038/s41612-024-00583-8, 2024.

Shalishe, A., Bhowmick, A., and Elias, K.: Meteorological drought monitoring based on satellite CHIRPS product over Gamo
Zone, Southern Ethiopia, Adv. Meteorol., 2022, 1–13, https://doi.org/10.1155/2022/9323263, 2022.

Sharma, M., Bangotra, P., Gautam, A. S., and Gautam, S.: Sensitivity of normalized difference vegetation index (NDVI) to
land surface temperature, soil moisture and precipitation over district Gautam Buddh Nagar, UP, India, Stoch. Environ. Res.
Risk Assess., 36, 1779–1789, https://doi.org/10.1007/s00477-021-02066-1, 2022.

Sheffield, J., Wood, E. F., and Roderick, M. L.: Little change in global drought over the past 60 years, Nature, 491, 435–438,
https://doi.org/10.1038/nature11575, 2012.

Smit, H. J., Metzger, M. J., and Ewert, F.: Spatial distribution of grassland productivity and land use in Europe, Agric. Syst.,
98, 208–219, https://doi.org/10.1016/j.agsy.2008.07.004, 2008.

Staten, P. W., et al.: Tropical widening: From global variations to regional impacts, Bull. Am. Meteorol. Soc., 101, E897–
E904, https://doi.org/10.1175/BAMS-D-19-0047.1, 2020.

Sun, J., Wang, X., Chen, A., Ma, Y., Cui, M., and Shilong, P.: NDVI indicated characteristics of vegetation cover change in
China's metropolises over the last three decades, Environ. Monit. Assess., 179, 1–14, http://dx.doi.org/10.1007/s10661-010-
1715-x, 2011.

Svoboda, M. D., and Fuchs, B. A.: Handbook of drought indicators and indices, Drought Water Crises: Integrating Science,
Management, and Policy, 155–208, https://doi.org/10.9781351967525, 2017.

Tall, M., Sylla, M. B., Dajuma, A., Almazroui, M., Houteta, D. N. K., Klutse, N. A. B., Dosio, A., Lennard, C., Driouech, F., Diedhiou, A., and Giorgi, F.: Drought variability, changes and hot spots across the African continent during the historical period (1928–2017), Int. J. Climatol., 43, 7795–7818, https://doi.org/10.1002/joc.8293, 2023.

Tian, F., Fensholt, R., Verbesselt, J., Grogan, K., Horion, S., and Wang, Y.: Evaluating temporal consistency of long-term global NDVI datasets for trend analysis, Remote Sens. Environ., 163, 326–340, https://doi.org/10.1016/j.rse.2015.03.014, 2015.

Tladi, T. M., Ndambuki, J. M., and Salim, R. W.: Meteorological drought monitoring in the Upper Olifants sub-basin, South Africa, Phys. Chem. Earth, 128, 103273, https://doi.org/10.1016/j.pce.2022.103273, 2022.

The NCAR Command Language (Version 6.6.2) Software: Boulder, Colorado: UCAR/NCAR/CISL/TDD, https://www.ncl.ucar.edu/Applications/spi.shtml. Last access: 11 June 2023.

Thom, H. C. S.: A note on the gamma distribution, Mon. Weather Rev., 86, 117–122, https://doi.org/10.1175/1520-0493(1958)086<0117:ANOTGD>2.0.CO;2, 1958.

Udmale, P., Ichikawa, Y., Manandhar, S., Ishidaira, H., and Kiem, A.: Farmers' perception of drought impacts, local adaptation and administrative mitigation measures in Maharashtra State, India, Int. J. Disaster Risk Sci., 10, 250–269, https://doi.org/10.1016/j.ijdrr.2014.09.011, 2014.

Vicente-Serrano, S. M., Domínguez-Castro, F., Reig, F., Tomas-Burguera, M., Peña-Angulo, D., Latorre, B., Beguería, S., Rabanaque, I., Noguera, I., Lorenzo-Lacruz, J., and El Kenawy, A.: A global drought monitoring system and dataset based on ERA5 reanalysis: A focus on crop-growing regions, Geosci. Data J., https://doi.org/10.1002/gdj3.178, 2022.

Vicente-Serrano, S. M., Gouveia, C., Camarero, J. J., Beguería, S., Trigo, R., López-Moreno, J. I., Azorín-Molina, C., Pasho, E., Lorenzo-Lacruz, J., Revuelto, J., Sanchez-Lorenzo, A., Garcia-Cediel, E., Ramos, P., and Lamela, M.: Response of vegetation to drought time-scales across global land biomes, Proc. Natl. Acad. Sci. U. S. A., 110, 52–57, https://doi.org/10.1073/pnas.1207068110, 2013.

Wilhite, D. A.: Drought as a natural hazard: Concepts and definitions. In Drought, A Global Assessment; Ed.; Routledge: London, UK, Volume I, pp. 3–18, https://doi.org/10.4324/9781315830896, 2000.

Wilks, D. S.: Statistical Methods in the Atmospheric Sciences, volume 91 of International Geophysics Series, Academic Press, Burlington, USA, 627 pp., ISBN: 0127519661, 2005.

Wright, J. S., Fu, R., Worden, J. R., Chakraborty, S., Clinton, N. E., Risi, C., Sun, Y., and Yin, L.: Rainforest-initiated wet season onset over the southern Amazon, *Proc. Natl. Acad. Sci.*, 114, 8481–8486, https://doi.org/10.1073/pnas.1621516114, 2017.

Xian, T., Xia, J., Wei, W., Zhang, Z.,Wang, R., Wang, L. P.,Ma, Y. F.: Is Hadley Cell expanding?, Atmosphere, 12, 1699, https://doi.org/10.3390/atmos12121699, 2021.

Yao, N., Li, Y., Lei, T., and Peng, L.: Drought evolution, severity and trends in mainland China over 1961–2013, Science of The Total Environment, 616-617, 73–89, https://doi.org/10.1016/j.scitotenv.2017.10.327, 2018.

Zhang, M., Wang, K., Liu, H., Yue, Y., Ren, Y., Chen, Y., Zhang, C., Deng, Z.: Vegetation inter-annual variation responses
660   to climate variation in different geomorphic zones of the Yangtze River Basin, China, Ecological Indicators, 152, 110357,
https://doi.org/10.1016/j.ecolind.2023.110357, 2023.

Zhao, Z., Zhang, Y., Liu, L. S., and Hu, Z.: The impact of drought on vegetation conditions within the Damqu River Basin,
Yangtze River Source Region, China, PLoS One, 13(8):e0202966, https://doi.org/10.1371/journal.pone.0202966, 2018.